#5159

A SIMPLE EMPIRICAL MODEL FOR PREDICTING VELOCITY DISTRIBUTIONS AND COMFORT IN A LARGE SLOT-VENTILATED SPACE

A.A. Fissore, Ph.D.

G.A. Liébecq, Ph.D.
Member ASHRAE

ABSTRACT

Large industrial or agricultural buildings are sometimes ventilated through slots along both sidewalls. In such situations, it is important to predict the internal climate in the occupied subzone of the building. Indoor air movements have been investigated on a reduced-scale model of a sheepfold. The study determined the parameters influencing jet pathways (Archimedes number and jet momentum), knowledge of which also yields the prediction of velocity distributions and temperature gradients in the occupied zone. If an average zone temperature is also known, comfort conditions can be determined. The model, however, was unable to predict vertical stratification in the whole internal space. Temperature and velocity measurements were also performed in the actual building, yielding a satisfactory validation of the model. The study can be considered as a first stage, demonstrating the possibility of developing such simple models. Results are only applicable to geometries similar to the one analyzed.

INTRODUCTION

The health and efficiency of workers in industrial halls are influenced by air and mean radiant temperatures, air velocity, and humidity. This is also valid for homeothermal animals, such as cattle, pigs, or sheep, where an adequate indoor climate is of prime importance for their health, growth, productivity, and reproduction.

Actually, many similarities exist between industrial and agricultural buildings. Very often, both are long and narrow, with a high triangular roof. They are generally ventilated through longitudinal slots along one or both lateral walls, with extraction at the vertex of the roof. Therefore, results of investigations on one type of building, and in particular studies on reduced-scale models, could reasonably be taken into consideration when analyzing the other.

The evaluation of comfort and health criteria is often deduced from estimates of mean velocities and temperatures in the occupied zone. However, available results in the literature emphasize the difficulty of accurately predicting those values. Therefore, this study is focused on determining the parameters influencing airflow patterns and temperature and velocity distributions in the occupied zone. It attempts to represent those phenomena by means of a simple model, whose accuracy is evaluated.

The study was carried out on a reduced-scale model of a sheepfold in laboratory conditions, and certain data in the actual building yield interesting comparisons.

Literature on the experimental investigation of indoor climates includes Jackman (1970), Hannay and Lebrun (1975), Fitzner (1981), Nielsen (1987), Larsson et al. (1987), and Sandberg and Blomqvist (1989) in residences. Satoshi (1987), Randall and Battams (1979), and Leonard and McQuitty (1986) published investigations on industrial or agricultural applications. All present useful information for the design of experiments and the analysis of results. None, however, could be related to the specific geometry considered here.

EXPERIMENTAL DESIGN

Description of the Model

Figure 1 shows a cross section of the laboratory setup. It is a model at one-third scale of a sheepfold. Geometrical similarity, however, is not respected at the top of the model, where the original triangular vertex of the prototype has been replaced by a rectangular casing, enabling the movement of a trailer carrying temperature and velocity sensors in the model. This modification, however, should not affect air movements in the occupied zone.

The front walls of the model are made of clear plastic for visualization of flows. The model was mounted inside a thermally controlled enclosure to maintain steady-state conditions during long periods.

Ventilation is provided by fans at inlets and outlets to maintain the same pressure inside and outside the model in order to minimize infiltration effects. The actual building is naturally ventilated. Therefore, in the model, wind-dominant effects will be reproduced by an inlet on one side only, low wind and stack effects by inlets on both sides. This

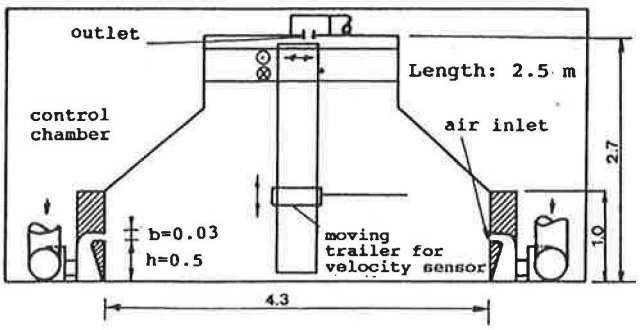

Figure 1 Section of the scale model

Adelqui A. Fissore is a Lecturer, Facultad de Ingenieria, University of Concepcion, Chile. **Georges A. Liébecq** is a Consulting Engineer at Econotec Consultants, Liege, Belgium. The present work was carried out at the Laboratory of Thermodynamics, University of Liege.

latter situation is also representative of a building with a fan at the roof exhaust. In all cases, the momentum of the air at inlets is assumed to be known.

Heat loads are provided by electrically heated panels located on the floor and on the roof. Panels on the floor represent the heat gains from animals in the occupied zone. On the inside surface of the roof, they simulate heat loads due to solar radiation.

Similarity Rules

It is well known that all similarity criteria appearing in the analysis of Navier-Stokes equations cannot be strictly satisfied simultaneously. Previous observations, notably Satoshi (1987), Leonard and McQuitty (1986), and Mierzwinski (1987), have confirmed that the most important condition of similitude is Archimedes number:

$$Ar_m = Ar_r,$$

as long as the Reynolds number remains above a critical value that was experimentally determined here (Fissore and Liébecq 1990):

$$Re_m > Re_c.$$

At the boundaries of the model, similitude is obtained by similar geometries and similar heat transfer rates. The latter condition is very difficult to satisfy properly and local similitude is applied: walls and laminar boundary sublayers are excluded from the modeled zone. In those conditions, heat transfers to that zone are only convective and similarity requires that the ratio of local convective heat transfer rates to the total convective heat transfer should be equal in reality and everywhere in the model. Such conditions can only be approached by maintaining nonheated surfaces at temperatures very close to the mean indoor air temperature and by heating only one (or two) wall(s) at a temperature well above indoor air.

Instrumentation

Thirty-three surface temperatures and 29 air temperatures (measured with shielded thermocouples) at fixed locations are recorded in the model. Considering all measurement errors, including radiative effects and reference point bias, the confidence interval of such measurements can be estimated at $\pm 0.2°C$.

Air velocities were measured by an omnidirectional, temperature-compensated, hot sphere probe. Here, errors are notably due to the effect of flow direction, natural convection resulting from probe heating, and integration time (between two and four minutes). A more detailed error analysis can be found in Fissore and Liébecq (1990), in which the following estimates for the confidence interval s_v on velocity V were derived:

$$s_v = 0.03 + 0.053\,V \text{ or } -(0.03 + 0.2\,V) \quad \text{for } V < 0.2 \text{ m/s}$$

or

$$s_v = \pm 0.11\,V \quad \text{for } V > 0.2 \text{ m/s},$$

the latter being reduced to $\pm 0.06\,V$ for strictly two-dimensional flows.

TEST PROCEDURES

Using an automatic positioning system, the anemometer and its associated thermocouple can be moved throughout the model. Two-dimensional flow is assumed and is verified before and after each test by smoke visualization in different cross sections. Therefore, measurements are mostly recorded in the median section of the model, where some 200 points are scanned. Steady-state conditions are maintained and regularly verified by fixed points of measurement. They present an average deviation in time of $\pm 0.12°C$, with a maximum observed at $\pm 0.3°C$.

Test conditions covered Reynolds numbers between 1,500 and 6,000 and Archimedes numbers up to 0.03, both being calculated on flow and geometry characteristics at air inlets.

Independence from the Reynolds number occurs only for $Re > 1{,}850$, as shown in Fissore and Liébecq (1990). In these experiments, all tests with $Ar > 0.02$ corresponded to Reynolds numbers between 1,500 and 1,850. Therefore, all correlations developed hereafter are applicable only for $Re > 1{,}850$ and $Ar < 0.02$ and, evidently, for the geometry considered.

Air was introduced from one or both sides, allowing the ratio of velocity in opposite inlets (F_v) to vary between 1 and ∞. Air exhaust occurred at the roof or through the opposite wall. The slot length (l) was varied from $l/L = 0.7$ to the total length of the model ($l/L = 1$).

Finally, two kinds of inlet velocity profiles were considered, corresponding to turbulence intensities of 3.5% and 9%.

LABORATORY RESULTS

Figure 2 shows an example of the velocities recorded. Values are given in percentage of the mean velocity at the inlet.

Figures 3a through 3d illustrate velocity fields in the lower part of the model, corresponding to the hatched area of Figure 2, for different test conditions. Values are obtained by linear interpolation of measurements and given in a linear scale between 0 (velocity = 0) and 9 (velocity at the inlet).

Figures 3a and 3b present velocity fields for one air inlet. In Figure 3a, both buoyancy and low-pressure effects (low pressure in the lower right corner due to entrainment by the air jet) cause the air jet to deflect strongly toward the floor. In Figure 3b, none of these effects occurs, the flow being isothermal. The ratio l/L being less than unity, the decrease of pressure due to entrainment is immediately compensated by the air moving perpendicularly to the plane of measurements. In those conditions, the jet tends to diffuse horizontally.

Figures 3c and 3d are representative of cases where air enters from both inlets and the ratio l/L is equal to unity. When Ar is significant (> 0.003) and inlets present similar momentum ($F_v < 1.3$), both jets deflect toward the floor and meet in the center of the zone (Figures 3c and 4a). This type of flow will be referred to as "type 2F."

On the other hand, for F_v less than 1.3, one jet is deflected toward the floor, while the other is directed upward along the roof (Figures 3d and 4b, flow type 1F1R). For low Ar and F_v, the flow becomes unstable and switches from type 2F to 1F1R without any change in boundary conditions.

Table 1 presents the various situations taken into consideration in this analysis. When two jets are present, the one presenting the largest Reynolds number is always

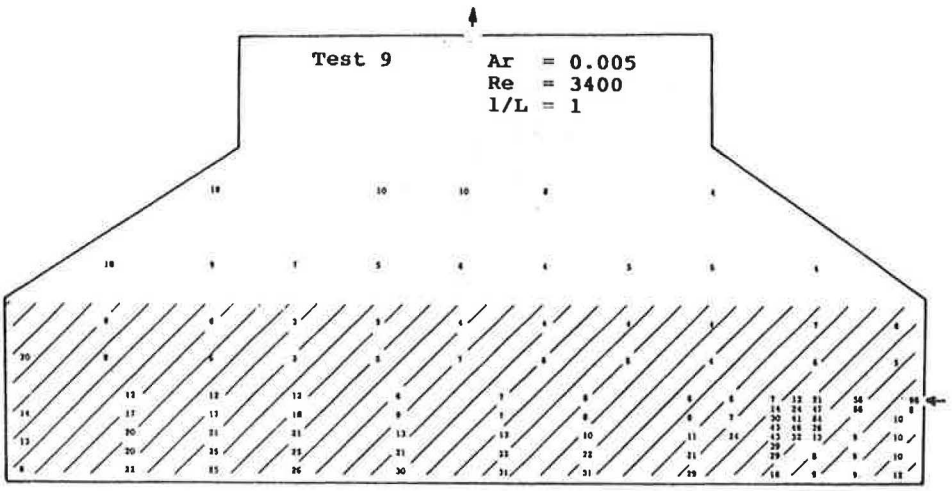

Figure 2 *Sample of velocity measurements in percentage of inlet velocity*

Figure 3a Test 9 Ar=0.005 l/L=1

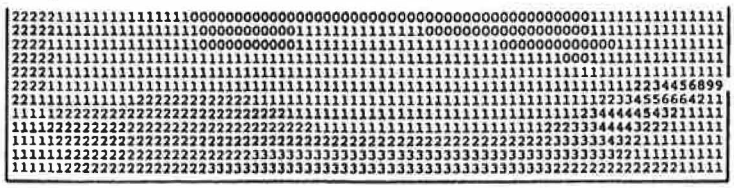

Figure 3b Test 27 Ar=0 l/L=0.86

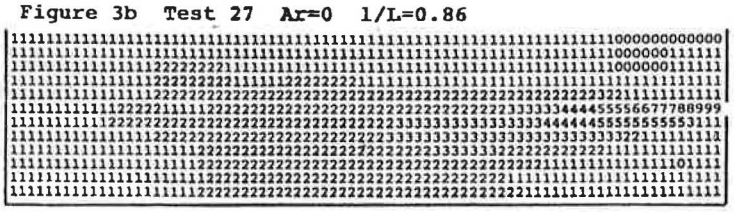

Figure 3c Test 24 Ar_1=0.0107 Ar_2=0.0086 l/L=1

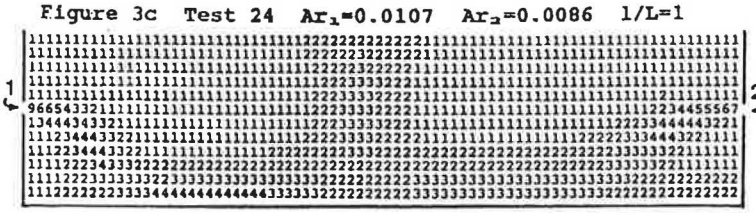

Figure 3d Test 19 Ar_1=Ar_2=0 l/L=1

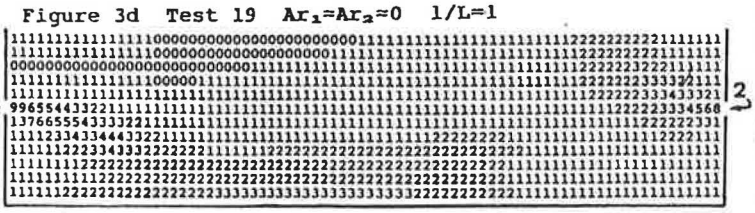

Figure 3 *Velocity fields in the lower part of the model (linear scale: 0 = velocity 0, 9 = inlet velocity)*

deflected toward the ground and its Archimedes number is used to select 2F or 1F1R patterns. Table 2 presents the F_v values of tests where two jets are present and the ratio *l/L* is equal to unity. Tests 19 and 22 are 1F1R-type flows, all others are 2F flows. Unstable flows could only be observed by smoke vizualizations and are not listed here.

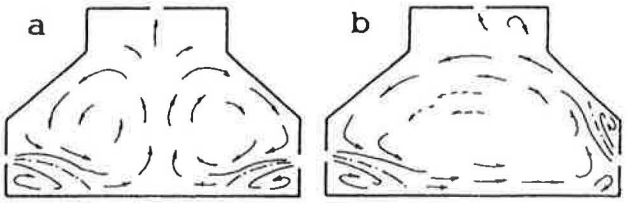

Figure 4 *Main types of flow patterns occurring with two inlets and l/L = 1*

The actual occupied zone, which extends to a height of 0.3 m, corresponds to the four bottom lines of Figures 3. In that region, airflows are obviously influenced by the jet patterns. It therefore becomes of prime importance to determine their location before any attempt is made to predict flow and comfort conditions in the occupied zone.

Jet Deflection

As already mentioned, jets can be deflected under the effect of a pressure difference or of buoyancy. In steady-state and isothermal conditions, several authors (Bourque and Newman 1960) have shown that the path of the deflected jet can be represented by a circle of radius *R* (see Figure 5). This deflection is due to a low-pressure region created between the jet, the floor, and nearby boundaries. It is understandably most obvious for slots along the whole side walls (*l/L* = 1) and practically disappears for *l/L* = 0.7, where the jet diffuses more or less horizontally (Figure 3b).

The influence of buoyancy is of similar importance. The literature generally suggests deflections following power law function of the distance away from the slot. Exponents proposed vary between 2.5 and 3 (Koestel 1955; Croome 1975).

When both effects combine, a circle path is an adequate representation (Fissore and Liébecq 1990). For *l/L* = 1 and Ar < 0.02, the radius of curvature becomes

$$\frac{R}{b} = 54 - 2200\,Ar \qquad s = 9 \qquad (1)$$

TABLE 1
List of Experimental Tests in the Reduced Scale Model

	l/L	Re_1	Re_2	Ar_1 *10^3	Ar_2 *10^3	*Qf* (W)	*Qr* (W)
1	1.00	-	1839	-	-2.5	0	0
2	1.00	1980		-0.3	-	0	0
3	1.00	-	2195	-	-0.6	0	0
4	1.00	-	3983	-	-0.1	0	0
5	1.00		4121		0.0	0	0
6	1.00	4179	-	-0.2	-	0	0
7	1.00	-	4480	-	2.3	2000	0
8	1.00	-	2755	-	3.0	600	0
9	1.00	-	3375	-	4.8	2030	0
10	1.00	2545	-	6.7	-	1700	0
11	1.00	2582	-	7.0	-	1850	0
12	1.00	2489	-	7.3	-	1700	0
13	1.00	-	2764	-	8.0	2020	0
14	1.00	2323	-	9.3	-	1900	0
15	1.00	2115	-	10.7	-	1700	0
16	1.00	-	1599	-	24.9	1700	0
17	1.00	-	2911	-	4.1	0	810
18	1.00	-	2370	-	5.9	0	815
19	1.00	2203	1830	-0.1	2.0	0	0
20	1.00	2218	2190	3.5	3.4	0	830
21	1.00	2554	2489	5.6	4.5	1900	0
22	1.00	2210	1725	7.6	13.2	1850	0
23	1.00	1951	2075	10.9	12.1	1350	830
24	1.00	1819	2337	10.7	8.6	1730	0
25	1.00	1474	1506	18.1	20.1	1870	0
26	0.86	-	2049	-	-0.5	0	0
27	0.86	-	5251	-	-0.1	0	0
28	0.86	-	4912	-	2.0	2000	0
29	0.86	-	3252	-	5.3	1960	0
30	0.86	-	2249	-	13.0	1900	0
31	0.86	3433	3853	0.0	0.0	0	0
32	0.70	-	3224	-	-0.1	0	0
33	0.70	-	2470	-	9.4	0	0

Legend:
l/L = Length of slot to length of model
Re_1 = Reynolds number in slot 1
Re_2 = Reynolds number in slot 2
Ar_1 = Archimedes number using slot 1 airflow characteristics
Ar_2 = Archimedes number using slot 2 airflow characteristics
Qf = Heat load on floor
Qr = Heat load on roof

Note: Negative Ar values can occur in the absence of heat load, when the jet air is slightly warmer than the indoor air.

where b is the vertical width of the air inlet and s measures the scatter about the regression line (standard deviation).

Mean Velocity in the Occupied Zone

The mean velocity of air in the occupied zone (V_m) is indeed influenced by those jets that are deflected toward the floor. It is, therefore, related to the momentum of air jets at the inlets. It is proposed to relate V_m to a fictitious global momentum velocity at the orifices (V_r),

$$V_r = 0.5\ V_{01}\ (1 + [1 + \frac{V_{02}^2}{V_{01}^2}]^{0.5}) \quad \text{(m/s)} \qquad (2)$$

TABLE 2
F_v-Values for Tests with Two Jets and *l/L* = 1

Test	F_v
19	1.33
20	1.11
21	1.13
22	1.40
23	1.03
24	1.16
25	1.07

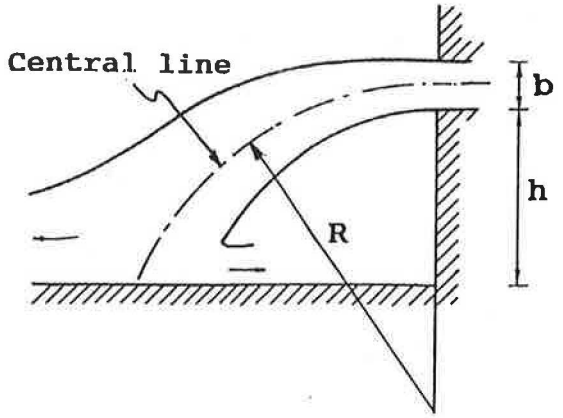

Figure 5 *Sketch of jet deflection toward the ground*

with V_{01} and V_{02} being averaged velocities at the slots. V_{02} will be nonzero only if both jets enter the occupied zone.

The occupied zone velocity is expressed as

$$V_m = k\,V_r \quad \text{(m/s)}. \tag{3}$$

Measurements show only a weak dependence upon the jet's radius of curvature and yield in first approximation,

$$k = 0.222.$$

A more refined model will nevertheless consider this influence. For one air inlet and $l/L = 0.86$, Figure 6 shows that a tendency is observable but with a high scatter in the results. It can be expressed by

$$k = 0.30 - 0.0191 \ln(R/b). \tag{4}$$

The mean velocity in the occupied zone depends indirectly on the Archimedes number. Only through the determination of R using Equation 1 does it have an influence.

Finally, the standard error for the calculation of V_m, considering the dispersion of the results, can be estimated as

$$s_{V_m}/V_r = 0.026.$$

Reduced Occupied Zone

A reduced occupied zone is also investigated. On the model, it is conventionally defined as the space below a height, 0.175 m, which corresponds to 0.55 m in the prototypical sheepfold.

This reduced zone is most appropriate when the laboratory setup is modeling large industrial buildings, say, some 30 m high. In that case, the reduced zone represents the model of an occupied zone of 1.8 m at a scale close to 1:10.

As illustrated in Figure 7, there is a direct relationship between mean velocities in the original occupied zone (V_m) and in the reduced one (V_{mr}):

$$\frac{V_{mr}}{V_m} = 1.404 - 0.0741 \ln \frac{R}{b} \tag{5}$$

$$s = 0.039.$$

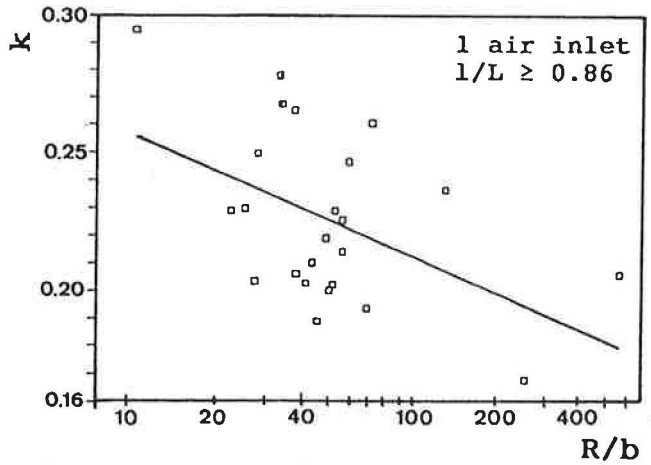

Figure 6 *Effect of radius of curvature on mean velocity in occupied zone ($k = V_m/V_r$)*

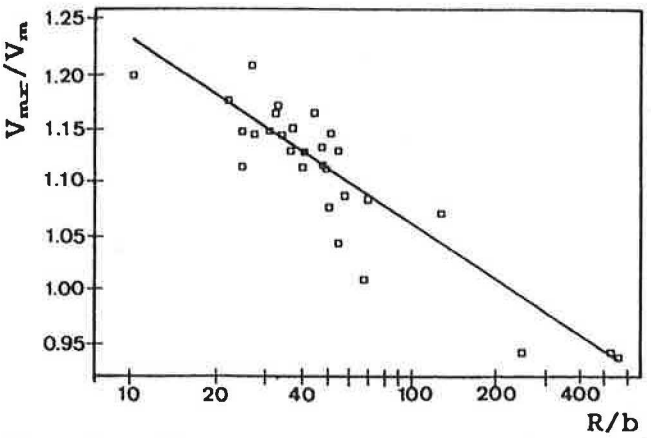

Figure 7 *Effect of radius of curvature on mean velocity in the reduced occupied zone*

Velocity Distribution around the Mean Value

In the occupied zone, the distribution of velocities around the mean value V_m can be characterized by the standard deviation:

$$SDEV = \left[\frac{\Sigma (V_i - V_m)^2}{N}\right]^{0.5}. \tag{6}$$

For one air inlet, the only observable dependence of this parameter occurs with the mean velocity, any other influence being weaker than the overall dispersion of experimental results (Figure 8):

$$SDEV = 0.33\ V_m. \tag{6'}$$

With both inlets used, the velocity distribution is more uniform, and the standard deviation becomes

$$SDEV = 0.30\ V_m. \tag{6''}$$

For both situations, the overall accuracy is measured by

$$s/V_r = 0.0053.$$

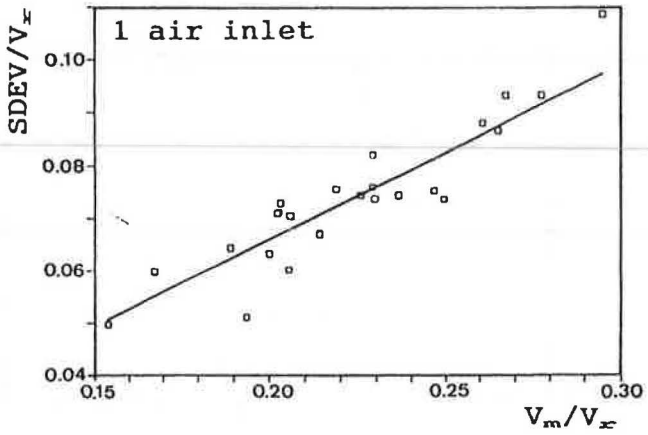

Figure 8 Velocity distribution vs. mean velocity in occupied zone

The standard deviation is a true characteristic of the dispersion only if the velocity distribution in space is Gaussian. Therefore, it is interesting to compare the actual distribution with that predicted by a Gaussian profile. Let V_g be the dimensionless variable:

$$V_{gi} = \frac{V_i - V_m}{SDEV}. \qquad (7)$$

The discrepancy between reality and Gaussian hypothesis is measurable through the standard error:

$$s_g = \left[\frac{\Sigma (f_{m,i} - f_{c,i})^2}{N}\right]^{0.5} \qquad (8)$$

where

$f_{m,i}$ = the cumulated frequency of V_{gi} obtained from measurements,

$f_{c,i}$ = that computed with the Gaussian assumption.

Figures 9a through 9c illustrate those considerations, presenting both cumulated frequencies vs. V_g. Figure 9a corresponds to a fair agreement (average s_g, 0.036), while Figure 9b shows the worst situation (s_g maximum) and Figure 9c the best (s_g minimum).

Temperature

Results of experiments show that the location of heat sources has no significant influence on the velocity field in the occupied zone. It has, however, a very important effect on thermal stratification. Any prediction of mean temperature in the occupied zone should take it into consideration as well as the inertia of the various walls. Furthermore, it has been impossible to relate the temperature of the occupied zone to any average value representative of the whole model. Therefore, simple models were unable to produce accurate predictions.

Nevertheless, if the mean temperature in the occupied zone is determined by any means, a reasonable prediction of the distribution around that mean value is feasible. Figure 10 shows some examples of temperature fields obtained by interpolation on measured quantities, in a similar manner as velocity fields were obtained in Figure 3.

Obviously, distributions of temperature in the occupied zone are influenced by jet paths and remain very similar to velocity distributions. This suggests that they could become independent of the location of heat loads, as velocity fields are.

This is actually confirmed by measurements. Tests were performed with heat sources on the ground, along the roof surface, or on both. In all cases, heat loads were varied in order to cover the range of Archimedes numbers between 0 and 0.02.

If T_m represents the mean temperature in the occupied zone and T_i the local temperature, a characteristic spatial standard deviation is

$$SDET = \left[\frac{\Sigma (T_i - T_m)^2}{N}\right]^{0.5} \quad (°C). \qquad (9)$$

This parameter is directly linked to the temperature difference between the occupied zone and the outdoors:

$$SDET = 0.116\,(T_m - T_o)\ (°C)$$
$$s = 0.0185\ (°C).$$

Quite normally, the temperature distribution is rather close to a Gaussian distribution, with a mean s_g on the order of 0.037 for all non-isothermal experiments.

Combined Sets of Temperature and Velocity

Comfort predictions depend upon the simultaneous determination of velocity and temperature at any location of the occupied zone. As high velocities (in the jet) correspond to low temperatures, the Gaussian assumption can associate those two quantities everywhere on a one-to-one basis but with opposite signs (see Figure 11).

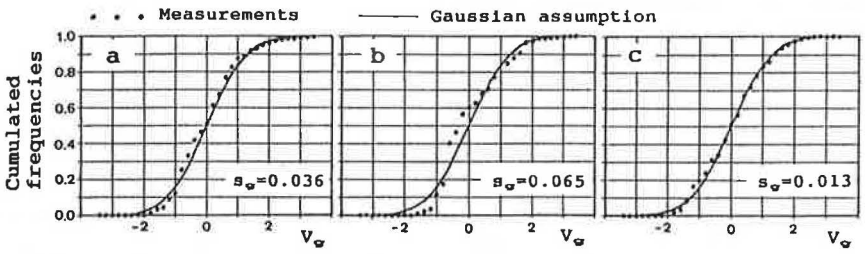

Figure 9 Test of Gaussian assumption

Figure 10a Test 9 Ar=0.005 l/L=1

Figure 10b Test 24 Ar_1=0.0107 Ar_2=0.0086 l/L=1

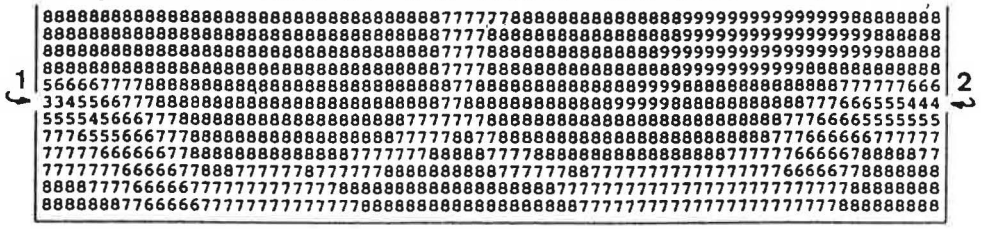

Figure 10 *Temperature distribution in the lower part of the model (linear scale: 0 = T_o, 9 = T_m)*

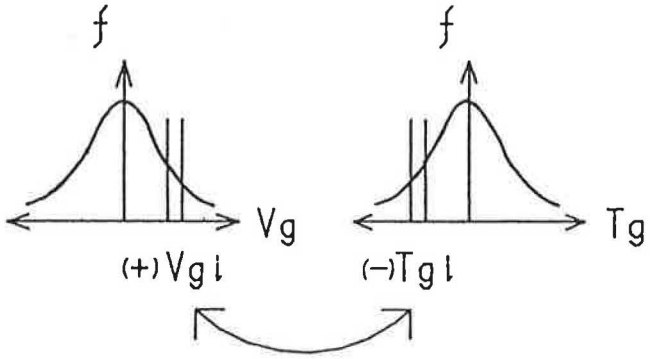

Figure 11 *Association of velocity and temperature within Gaussian assumption*

As the predicted mean vote (PMV) constitutes a useful indicator for combined velocity and temperature effects, it has been used to verify the above-mentioned argument. Cumulated PMV frequencies have been computed using directly measured data and compared with data obtained from Gaussian laws. For all non-isothermal experiments, the agreement yields a mean standard error of $s_e = 0.04$.

DIRECT APPLICATION

Equations 1 through 4 can be used to predict mean velocity values (V_m) in the occupied zone of the actual sheepfold from the knowledge of the air velocities at the inlets and of a representative temperature in the building. Reynolds and Archimedes numbers are determined first. When two jets are observed, F_v is computed (for instance, as the ratio of Reynolds numbers if slots are strictly similar) and three situations can occur:

1. If F_v is larger than 1.3, the jet presenting the lowest value of Re is deflected toward the roof.
2. If F_v is lower than 1.3 but both Archimedes numbers exceed 0.003, both jets are deflected toward the floor.
3. If F_v is lower than 1.3 but one value of Ar is below 0.003, the flow pattern is unpredictable. Those conditions, however, are seldom encountered in natural ventilation, because $F_v = 1$ occurs mainly when there is no wind. In that case, inlet velocities are low and the Archimedes number is large. Indeed, in the measurements realized on site and mentioned hereafter, critical values of Ar and F_v were only met 0.5% of the time.

As an example, Figure 12 presents velocity predictions in the occupied zone when

$$l/L = 1$$
$$Ar = 0.002$$

yielding, through Equation 1,

$$R/b = 50.$$

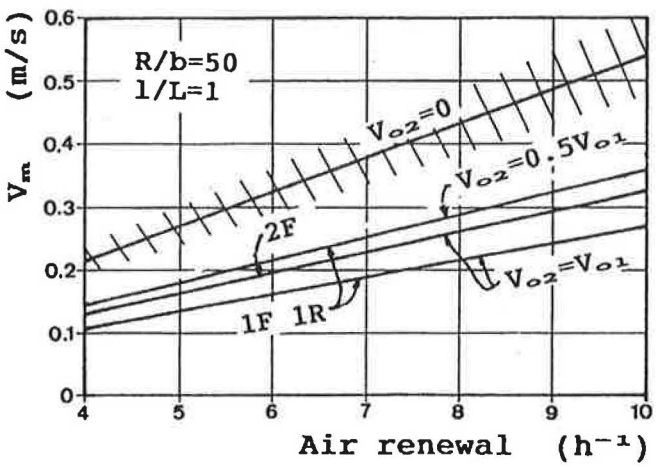

Figure 12 *Mean velocity prediction for different air renewal rates*

For various air renewal rates, three types of inlet conditions are considered:

- one inlet only ($V_{02} = 0$);
- two inlets with equal momentum ($V_{02} = V_{01}$), unpredictable flow pattern;
- two inlets with $V_{02} = 0.5\ V_{01}$, situation 1F1R.

When both inlets present similar momentum, situations 1F1R and 2F could be met. The difference observed between both predictions amounts to approximately 17%.

For illustrative purposes, the hatched area around the curve for one inlet (case 1) indicates the confidence interval ($\pm s$) of the correlation yielding the mean velocity V_m.

Figure 13 was obtained using Equations 1 through 4, Equation 6′ for *SDEV*, and the assumption of a Gaussian distribution. It indicates the relative volume of the occupied zone experiencing velocities within a given range when one inlet only is operating. For instance, for an air renewal of 5 (volumes/hour), 12.5% of the occupied zone is underventilated (velocity below 0.2 m/s), while 5% experiences velocities higher than 0.5 m/s.

VALIDATION IN THE REAL BUILDING

Previous estimates produced by the sample model have been compared to measurements performed on the prototypical sheepfold. Slight differences between the geometry of the building and that of the model have already been mentioned. They should not affect the velocity field in the occupied zone.

More important differences appear due to air movements inside and around the building. First, large parasitic air infiltrations were detected in the sheepfold. Second, fluctuations in wind speed and direction and nonuniform pressure distributions on the walls and particularly along the ventilation slots (Aynsley 1989) created flows not strictly two-dimensional inside the building. Third, obstacles are present inside the building. Further minor differences could be produced by slightly different heat exchanges at the walls in the prototype and in the model.

Velocity values were compared in the reduced-size occupied zone. Measurements were performed at four fixed locations selected to represent adequately the average velocity. Measurements also included velocity at inlets and numerous temperatures inside and outside. The investigation

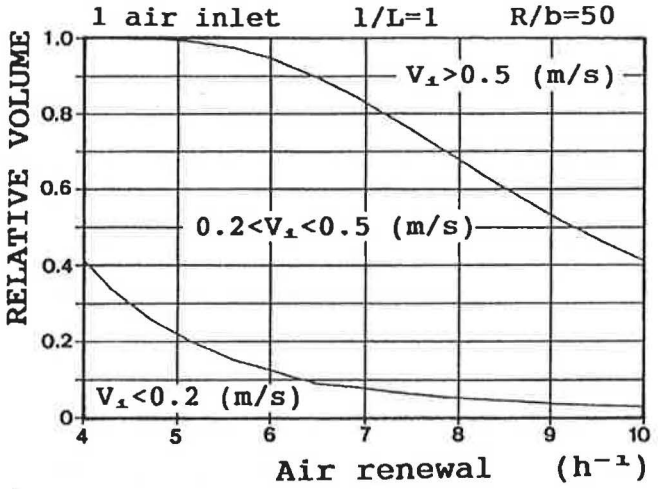

Figure 13 Volume fraction within prescribed velocity range for different air renewal rates

occurred during 10 days in mid-season and recordings were done every five minutes.

Rigorous comparison with model predictions can only be performed for large Reynolds numbers (Re > 1,850) and Ar < 0.02. During measurement periods, the first condition is respected 95% of the time, while Ar < 0.02 is only encountered 50% of the time. Assuming all sets of measurements to represent stabilized situations, thus independent from each other, all recordings not satisfying both conditions are eliminated. In those conditions, the comparison between predictions using the model and actual measurements on site yields a standard deviation:

$$\frac{s}{V_r} = \left[\frac{\Sigma((V_{mr,m}/V_r) - (V_{mr,c}/V_r))^2}{N}\right]^{0.5} = 0.056$$

where

$V_{mr,m}$ = mean velocity in the reduced occupied zone obtained from measurements,

$V_{mr,c}$ = obtained by application of Equation 5.

This value slightly decreases (to 0.051) if hourly mean values are used instead. This corresponds approximately to twice the dispersion of experimental results in the laboratory setup.

DISCUSSION AND CONCLUSIONS

The present work constitutes an attempt to develop a simple empirical model able to predict velocity and temperature distributions in the occupied zone of a large building with ventilation through slots.

For the range of Archimedes numbers considered in this study, airflow patterns inside the building are mainly influenced by the development of jets issued from ventilation slots. Their pathways are influenced by the formation of low-pressure zones between the jet boundary and nearby walls and by buoyancy.

Simple modeling takes into account effects of slot length compared to the building length (l/L), relative velocities at inlets (F_v), and the Archimedes number (Ar). It can predict velocity and velocity distribution in the occupied zone of the building. It fails to produce an estimate of the mean temperature in the occupied zone, because it is unable to consider thermal stratification and effects of wall inertia. However, temperature distributions around the mean are predictable, because they are again in direct connection with jet pathways.

Airflow rates entering the building by the effect(s) of wind and/or stack can be computed by classical methods, involving notably the consideration of pressure coefficients on the envelope of the building. On the other hand, building load computer programs can predict indoor temperatures representative of the mean temperature of the occupied zone. With the results of those calculations, the simple model can now produce the value of the variables determining environmental conditions in the occupied space. It could easily be implemented into a building loads program.

Evidently, results of the investigation can only be applied to buildings that are similar to the model considered, but measurements on site have shown that the reduced-scale approach is adequate in those conditions.

The scattering of experimental results being due to phenomena not modeled, it represents a means of estimating the accuracy of the present approach. It is, therefore,

observed that the mean velocity in the occupied zone (V_m) is predicted with a standard error of some 12% (this corresponds to 2.6% of the reference velocity V_r). The velocity distribution around the mean (*SDEV*) is predicted with an accuracy of 2.5% of V_m, while the index of temperature distribution (*SDET*) has a probable error of 2% of the temperature difference between indoors and outdoors.

Evidently, larger differences occur when comparing predictions by the model with on-site measurements. The present attempt yields a prediction with an accuracy of 5% of V_r, thus twice the error deduced from laboratory measurements. This is probably due mainly to parasitic ventilation effects, but remains very satisfactory for practical applications.

NOMENCLATURE

b	=	vertical width of air inlet (m)
F_v	=	velocity ratio, $F_v = V_{01}/V_{02}$, with $V_{01} > V_{02}$
h	=	height of location of air inlet (m)
k	=	dimensionless factor, $k = V_m/V_r$
L	=	length of transverse walls supporting air inlets (m)
l	=	length of air inlet (m)
R	=	radius of curvature of the jet (m)
s	=	standard deviation
SDEV	=	space standard deviation of velocity (m/s)
SDET	=	space standard deviation of temperature (°C)
s_g	=	deviation from Gaussian law (Equation 8)
T_g	=	dimensionless Gaussian temperature, $T_{gi} = ((T_i - T_o) - (T_m - T_o))/SDET$
T_i	=	local temperature (°C)
T_m	=	mean temperature in occupied zone (°C)
V_i	=	local air velocity (m/s)
V_m	=	mean velocity in the occupied zone (m/s)
V_mr	=	mean velocity in the reduced occupied zone (m/s)
V_r	=	fictitious reference velocity (m/s)
V_g	=	dimensionless Gaussian velocity, $V_{gi} = (V_i - V_m)/SDET$
V_{01}, V_{02}	=	velocities at air inlets with $V_{01} > V_{02}$ (m/s) = cinematic viscosity (m^2/s)

Subscripts

c	=	critical
m	=	model
o	=	inlet conditions
r	=	reference or real building
1, 2	=	inlet numbers

Nondimensional Numbers

Ar	=	Archimedes number, $Ar = g\,\beta\,(T_m - To)\,b/V_{o2}$
Re	=	Reynolds number, $Re = V_{o2}\,b/\nu$

BIBLIOGRAPHY

Aynsley, R.M. 1989. "The estimation of wind pressures at ventilation inlets and outlets on buildings." *ASHRAE Transaction*, Vol. 95, Part 2.

Bourque, C., and B.G. Newman. 1960. "Reattachment of a two-dimensional incompressible jet to an adjacent flat plate." *The Aeronautical Quarterly*, Vol. XI.

Croome, D.J. 1975. *Air conditioning and ventilation of buildings*. Oxford: Pergamon Press.

Fissore, A., and G. Liébecq. 1990. "Experimental study of air jets pathways in large slot ventilated spaces." ROOM-VENT '90, Engineering Aero- and Thermodynamics of Ventilated Rooms, Oslo.

Fitzner, K. 1981. "Airflow experiments in full-scale rooms." *ASHRAE Transactions*, Vol. 87, Part 1, pp. 1143-1153.

Hannay, J., and J. Lebrun. 1975. "Efficiency of induction and fan coil units for summer operation." *Proc. Clima 2000*, Milan, Vol. 2.

Jackman, P.J. 1970. "Air movements in rooms with sidewall mounted grilles. A design procedure." The Heating and Ventilating Research Association, Laboratory Report No. 65, Bracknell, England.

Koestel, A. 1955. "Paths of horizontally projected heated and chilled air jets." *ASHVE Transactions*, Vol. 61, pp. 213-233.

Larsson, B., K. Neikter, and O. Strindehag. 1987. "Air distribution efficiency in clean rooms." ROOM VENT-87, Air Distribution in Ventilated Spaces, Stockholm.

Leonard, J.J., and J.B. McQuitty. 1986. "The use of Archimedes number in the design of ventilation systems for animal housing." Conference on Agricultural Engineering, Adelaide.

Mierzwinski, S. 1987. "Some experiences in air distribution research." ROOM VENT-87, Air Distribution in Ventilated Spaces, Stockholm.

Nielsen, P.V. 1987. "Measurements on buoyant wall jet flows in air conditioned rooms." ROOM VENT-87, Air Distribution in Ventilated Spaces, Stockholm.

Randall, J.M., and V.A. Battams. 1979. "Stability criteria for airflow patterns in livestock buildings." *J. Agric. Engng. Res.*, Vol. 24, pp. 361-374.

Sandberg, M., and C. Blomqvist. 1989. "Displacement ventilation systems in office rooms." *ASHRAE Transactions*, Vol. 95, Part 2.

Satoshi, T. 1987. "Scale model experiment of air distribution in the large space of the Shinkokuikan sumo wrestling arena." ROOM VENT-87, Air Distribution in Ventilated Spaces, Stockholm.